PHILOSOPHICAL TRANSACTIONS OF THE ROYAL SOCIETY A MATHEMATICAL, PHYSICAL & ENGINEERING SCIENCES

Atoms in micron-sized metallic and dielectric waveguides

E. A. Hinds, K. S. Lai and M. Schnell

Phil. Trans. R. Soc. Lond. A 1997 **355**, 2353-2365
doi: 10.1098/rsta.1997.0132

Atoms in micron-sized metallic and dielectric waveguides

By E. A. Hinds[1], K. S. Lai[1,2] and M. Schnell[1,3]

[1]*Sussex Centre for Optical and Atomic Physics, University of Sussex, Falmer, Brighton BN1 9QH, UK*

[2]*Sloane Physics Laboratory, Yale University, 217 Prospect Street, New Haven, CT 06520, USA*

[3]*Fakultät für Physik, Universität Konstanz, Universitätsstr. 10, Postfach 5560, 78434 Konstanz, Germany*

Over the past ten years, our group has investigated the effects of confinement on atoms inside metallic micron-sized cavities in order to elucidate some basic phenomena in the field of cavity quantum electrodynamics (QED). The first of these was the inhibition of spontaneous emission from an atom inside a cavity. This was followed by a laser spectroscopic measurement of the van der Waals interaction between a single Rydberg atom and a gold cavity, which showed that a simple electrostatic model of the atom–cavity interaction is correct when the cavity is small enough. More recently, the retarded Casimir–Polder force was measured between a ground state sodium atom and a large cavity, demonstrating that the van der Waals potential fails at long enough range and that the vacuum fluctuations of the field then have an important role in the interaction of the atom with the cavity. Our group is now pushing forward these investigations to study cavities whose walls have losses and dispersion, where the theory of cavity QED is significantly more complicated. With real surfaces, we have to deal with the complex dielectric response $\varepsilon(\omega)$ of the material, which exhibits frequency-dependent absorption and dispersion. One particularly interesting case is when a downward transition in the atom is resonant with an excitation of the cavity walls. This opens a new branch for the atomic decay: as an alternative to creating a photon within the space surrounded by the cavity walls the atomic decay can now create an electromagnetic excitation of the walls themselves. Another novel feature of our experiments is that the Bohr frequencies of the atom are close to the k_T/h, where T is room temperature. We therefore expect to be able to measure effects associated with QED at finite temperature; in other words, to study how the blackbody radiation affects our experiments. By conducting experiments with real surfaces, we hope to elucidate and perhaps simplify the theoretical models used to describe these systems.

1. Introduction

Charged particles are inescapably coupled to the electromagnetic radiation field. Even in a vacuum, an atom is perturbed by electromagnetic quantum noise (vacuum fluctuations) and this coupling is responsible for some basic phenomena such as the Lamb shift and spontaneous radiative decay. These radiative effects can be calculated

Phil. Trans. R. Soc. Lond. A (1997) **355**, 2353–2365
Printed in Great Britain

using quantum electrodynamics (QED) and for cases when the atom is in free space, remarkable agreement has been found between theory and experiment. If the atom is in the vicinity of conducting or dielectric material, the electromagnetic field is perturbed and the radiative properties of the atom can sometimes be substantially modified. This area of physics—the study of electromagnetic fields restricted to a space with boundaries and the radiative properties of atoms in such a field—is called *cavity quantum electrodynamics*. Inside a cavity or waveguide, the spectrum of the electromagnetic field modes is strongly modified for wavelengths that are comparable with, or longer than, the physical dimensions. Thus, it is possible by a suitable choice of cavity geometry to change the spectrum and spatial distribution of electromagnetic quantum noise in a well-defined way and hence control both the Lamb shift and spontaneous decay rate. The possibility of modifying spontaneous emission rates was first mentioned by Purcell (1946). A detailed cavity QED calculation of the force between an atom and a conducting plate was made by Casimir & Polder (1948) and was soon extended (Casimir 1948) to the force between two conducting plates. There followed a large number of papers, nearly all theoretical, concerning the radiative rates and level shifts of atoms near conducting surfaces. There have also been a few experiments which have now demonstrated the existence of all the basic cavity QED phenomena predicted for perfect metallic cavities (see, for example, the review article by Hinds (1994), the book edited by Berman (1994) and the recent experiment by Lamoreaux (1997)).

Our group, previously at Yale University and now at Sussex, has studied the inhibition of spontaneous emission in a metallic cavity. We have also measured the dispersive (non-resonant) coupling between an atom and a cavity in two limiting cases: the short-range, non-retarded van der Waals interaction (Sandoghdar 1992) and the long-range, retarded Casimir–Polder interaction (Sukenik *et al.* 1993). The next section is an account of these experiments in (almost) perfect metallic cavities. It is followed in § 3 by a discussion of near-field cavity QED with imperfect surfaces that exhibit absorption and dispersion. In § 4 we look at spontaneous emission near several real surfaces and show that Rydberg atoms can be strongly coupled to ionic crystals through their surface polariton modes. In § 5 we see how the energy levels of an atom close to such a surface are perturbed by the coupling to the surface resonance; and finally in § 6 we discuss the implications of finite temperature, since hitherto we have assumed $T = 0$ K.

2. Cavity QED with perfect conductors

The apparatus we are using varies from one experiment to another, but the basic ingredients, shown in figure 1, are an effusive beam of alkali atoms (Na, Rb or Cs) and a parallel-plate cavity a few millimetres long and roughly 1 μm wide, formed by two rectangular metal or dielectric mirrors. The atoms can be excited, by means of two lasers, to a Rydberg level (typically $n = 10$–30) which is then field ionized and counted using a channel electron multiplier. The lasers can be positioned to excite the atoms before entering the cavity, within the cavity, or after leaving the cavity, depending on the experiment. Inside the parallel-plate microcavity, the fluctuations of the quantized radiation field are strongly modified for wavelengths comparable with the plate spacing. This changes both the spontaneous emission rate of an excited atom and the self energy of an atomic level. Since the energy level shifts are position

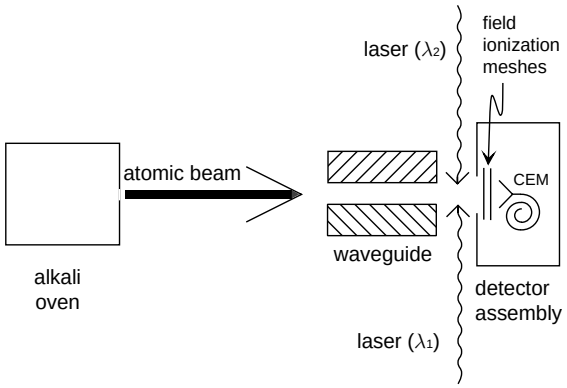

Figure 1. Schematic diagram of experimental set-up. A beam of alkali atoms passes through a parallel plate waveguide, which is coated with the surface of interest. Two laser beams (wavelengths λ_1 and λ_2) promote the atom by stepwise excitation to a Rydberg level which is detected by field ionization in front of a channel electron multiplier. Each laser beam can be positioned before, inside, or after the waveguide to allow studies of lifetime, level shift or deflection.

dependent, there are also forces between the atom and the cavity walls; these are the van der Waals and Casimir–Polder forces.

Although the idea of modified spontaneous emission is an old one, it was not demonstrated in a quantum system until Drexhage (1974) showed that the fluorescence from dye molecules is modified when they are placed near a surface. More recently, it became possible to control the spontaneous emission from single atoms coupled to well-defined cavities and, for example, to induce a strong anisotropy as demonstrated by our group (Jhe *et al.* 1987). In that experiment, we suppressed the spontaneous decay of caesium atoms from $5D_{5/2}$ to $6P_{3/2}$ at 3.49 μm by placing them between parallel plates 1.1 μm apart. The radiation field is unable to propagate in this parallel-plate waveguide when the electric field is parallel to the walls because the wavelength is longer than twice the plate spacing: the frequency is below the waveguide cut-off. Consequently, the excited atoms are unable to radiate with this polarization. In our experiment, the caesium atoms from the oven were prepared in the $5D_{5/2}$ ($F = 4$, 5 and 6) state by laser excitation before entering a gold coated parallel-plate cavity 1.1 μm wide and 8 mm long. Their flight through the cavity lasted 13 natural lifetimes, but even so a significant fraction of them emerged still in the $5D_{5/2}$ state, as shown in figure 2. These were the atoms in $F = 6$, $m_F \pm 6$, which can only decay by emitting photons polarized parallel to the mirrors. The other m_F sublevels decayed rapidly indicating a strong anisotropy of the vacuum field in the waveguide.

The idea that the cavity also affects the self energy of an atom is also rather old (Casimir & Polder 1948) and similarly escaped experimental verification for many years until Heinzen & Field (1987) saw the resonance line of barium shift when the atoms were coupled to a resonant cavity. This effect can be viewed as just the frequency pulling that occurs whenever two oscillators are coupled to each other; the interesting point is that one of the oscillators is a single atom. Our group measured the non-resonant coupling between an atom and a cavity in two limiting cases: the short-range, non-retarded van der Waals interaction (Sandoghdar *et al.* 1992) and the long-range retarded Casimir–Polder interaction (Sukenik *et al.* 1993).

If an atom in state $|a\rangle$ is sufficiently close to a plane perfectly conducting mirror,

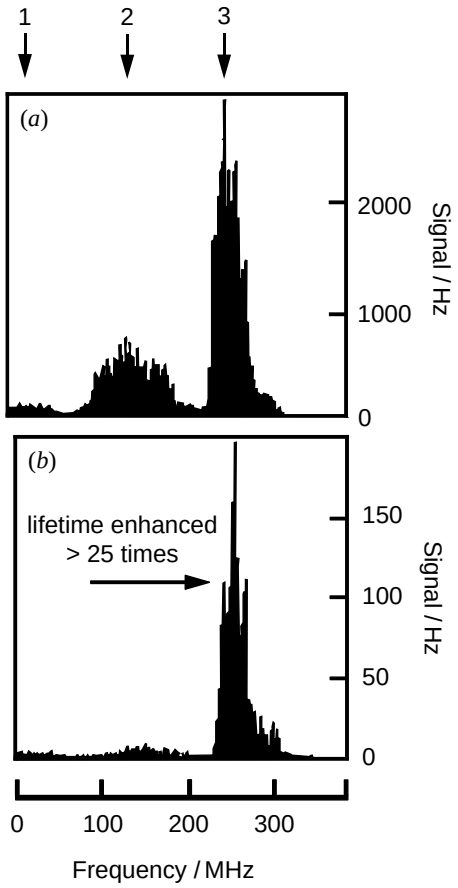

Figure 2. Spectra of the Cs($5D_{5/2} \rightarrow 26F$) transition taken from Jhe *et al.* (1987). (*a*) With atoms excited to the $5D_{5/2}$ state after leaving the cavity. (*b*) With atoms excited to the $5D_{5/2}$ state before entering the cavity. Labels 1, 2 and 3 correspond to the $5D_{5/2}$ $F = 4$, 5 and 6 hyperfine levels, respectively. The strong enhancement of the $F = 6$ peak relative to the others in their spectrum demonstrates the inhibition of decay from the $m_F = \pm 6$ levels as a result of the waveguide cut-off.

the van der Waals interaction energy is given by the simple Lennard–Jones formula

$$\Delta_{\mathrm{vdW}} = -\frac{1}{4\pi\varepsilon_0}\frac{\langle a|d_\rho^2 + 2d_z^2|a\rangle}{16z^3}, \tag{2.1}$$

where d_ρ and d_z are the components of the atomic dipole moment parallel and perpendicular to the surface of the mirror. This can be understood as the self-interaction between the fluctuating dipole moment of the atom and its instantaneous images in the cavity walls. For the parallel-plate geometry which we have in our experiment, we need to sum over all the image dipoles, resulting in a van der Waals shift at the centre of a cavity of width L given by

$$\Delta_{\mathrm{vdW}} = -\frac{\zeta(3)}{4\pi\varepsilon_0}\frac{\langle a|3d_\rho^2 + 8d_z^2|a\rangle}{4L^3}, \tag{2.2}$$

where the Riemann zeta function $\zeta(3)$ is approximately 1.2. This instantaneous van der Waals limit is valid as long as the time it takes the electromagnetic field to prop-

Figure 3

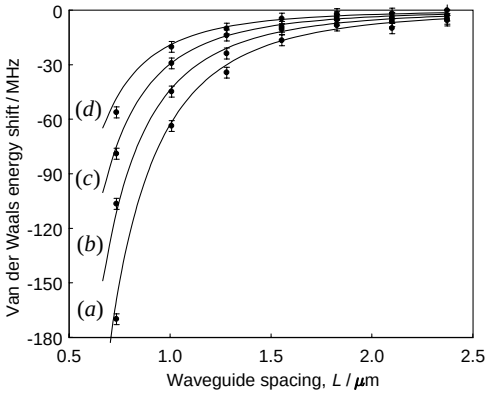

Figure 4

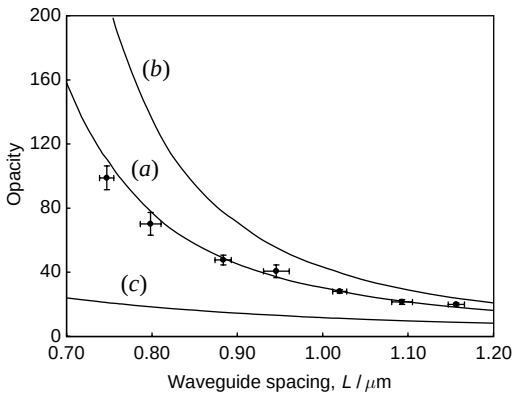

Figure 3. Dots show measured energy level shifts versus waveguide width L for sodium atoms midway between gold plates (from Sandoghdar *et al.* 1992). The four series (a)–(d) correspond to states 13S–10S, respectively. Lines show shifts calculated using the instantaneous van der Waals potentials of equation (2.2). The agreement with experiment shows that the simple model is a good approximation when the waveguide spacing is small.

Figure 4. Opacity of parallel-plate gold waveguide for ground state sodium atom versus plate spacing taken from Sukenik *et al.* (1993). Opacity is defined as $I(6\ \mu\mathrm{m})/I(L)$, where $I(L)$ is the intensity of the transmitted atomic beam as a function of spacing L. Curves show theoretical opacities for various assumed atom–cavity interaction potentials. (a) QED interaction (equation (2.3)); (b) van der Waals interaction (equation (2.2)); (c) no interaction. The experiment clearly supports the QED potential which is mainly in the fully retarded Casimir–Polder regime.

agate from the atom to the mirror and back is much shorter than the characteristic fluctuation time of the electric dipole moment, which means that the wavelengths of the strong dipole transitions must be much larger than the atom–mirror distance.

The experiment was performed on sodium Rydberg atoms (n = 10, 11, 12, 13) whose strong dipole transitions have wavelengths of order 100 μm, certainly much larger than the mirror spacing of a few μm. The interaction energy was measured by exciting atoms inside and outside the cavity and comparing the excitation spectra to determine the shift. By varying the gap width (L) of the waveguide and doing the experiment on states of different quantum number n, the van der Waals energy shift was verified, including the $1/L^3$ and $\langle d^2\rangle$ dependence as shown in figure 3.

At the other extreme, when the atom is much further from the surface than its characteristic wavelengths, the interaction is no longer a near-field effect and quantum fluctuations of the field become important. The theoretical problem of an atom between parallel plates has been analysed quite fully (for an excellent recent account see Barton (1987*a*,*b*)). In general, the position-dependent atom–cavity interaction potential is quite complicated to write down explicitly. For a spherical atom in ground state $|g\rangle$, the following form is more appealing than most:

$$\Delta_{\mathrm{QED}} = -\sum_e \frac{\pi\langle e|\boldsymbol{d}|g\rangle|^2}{6\varepsilon_0 L^3}\int_0^\infty \mathrm{d}\rho\,\frac{\rho^2\cosh(2\pi\rho z/L)}{\sinh(\pi\rho)}\tan^{-1}\left(\frac{\rho\lambda_{eg}}{2L}\right), \tag{2.3}$$

where z is the distance of the atom from the cavity centre, L is the waveguide spacing and λ_{eg} is the wavelength of the e–g transition. For the case when $\lambda_{eg} \gg L$, we recover the van der Waals limit given in equation (2.2). At the opposite extreme, the regime of Casimir & Polder when $\lambda_{eg} \ll L$, equation (2.3) is well approximated

by the Casimir–Polder potential

$$\Delta E_{\mathrm{CP}} = -\frac{1}{4\pi\varepsilon_0}\frac{\pi^3\hbar c\alpha_{\mathrm{stat}}}{L^4}\left(\frac{3-2\cos^2(\pi z/L)}{8\cos^4(\pi z/L)}\right). \tag{2.4}$$

where α_{stat} is the scalar static electric polarizability, defined as

$$\frac{2}{3}\sum_e |\langle g|\boldsymbol{d}|e\rangle|^2/(E_e - E_g),$$

and E_e and E_g are the energies of the unperturbed atomic states $|e\rangle$ and $|g\rangle$. This energy shift is most naturally understood as a change in the Lamb shift resulting from the modified vacuum fluctuations in the presence of the cavity.

In our experiment we studied the deflection of ground state sodium atoms passing through our micron-sized parallel-plate cavity by measuring the intensity of the transmitted ground state sodium atomic beam as a function of the cavity width. The expected transmission through the long narrow channel, or more precisely its inverse, the 'opacity', is plotted in figure 4 for the cases of Casimir–Polder potential (a), van der Waals potential (b), and no potential (c). The experimental results verified that the Casimir–Polder potential predicted by QED is the correct one.

In all the experiments above, the cavity walls could be regarded as simple frequency-independent boundary conditions because they were very good conductors. Now we are investigating cavities made with dielectric surfaces which are not so simple.

3. Cavity QED with imperfect surfaces

Let us recall that in electrostatics the effect of a thick slab of material on a charge q at distance z from its surface can be modelled by placing a fictitious image charge $-q(\varepsilon-1)/(\varepsilon+1)$ at $-z$, where ε is the static dielectric constant of the material. Similarly, the effect of a dielectric half-space on an electric dipole $\boldsymbol{d}$ is equivalent to an image dipole whose components parallel and perpendicular to the surface are $\boldsymbol{d}_\rho^{\mathrm{image}} = -(\varepsilon-1)/(\varepsilon+1)\boldsymbol{d}_\rho^{\mathrm{image}}$ and $\boldsymbol{d}_z^{\mathrm{image}} = (\varepsilon-1)/(\varepsilon+1)\boldsymbol{d}_z^{\mathrm{image}}$. Hence the van der Waals energy shift of an atom in front of a dielectric surface, derived from the instantaneous dipole–dipole interaction, is given by

$$\Delta E_{\mathrm{vdW}} = -\frac{\varepsilon-1}{\varepsilon+1}\frac{\langle a|d_\rho^2 + 2d_z^2|a\rangle}{64\pi\varepsilon_0 z^3}. \tag{3.1}$$

The case of a perfect mirror, equation (2.1), is recovered in the limit of large ε. This simple model assumes that the dielectric constant ε is frequency independent but, of course, the real world is much more interesting than that; the dielectric constant depends on frequency because of resonances in the medium.

A more general formula for the van der Waals interaction between an atom and a half-space with dielectric function $\varepsilon(\omega)$ was derived by McLachlan (1963):

$$\Delta E_{\mathrm{dispersion}} = -\frac{1}{4\pi\varepsilon_0}\frac{1}{16z^3}\frac{2}{\pi}\int_0^\infty \mathrm{d}\xi\left(\frac{\varepsilon(\mathrm{i}\xi)-1}{\varepsilon(\mathrm{i}\xi)+1}\right)\sum_n \frac{\omega_{na}}{\omega_{na}^2+\xi^2}[|d_\rho^{na}|^2 + 2|d_z^{na}|^2], \tag{3.2}$$

where ω_{na} is the atomic transition frequency $(E_n - E_a)/\hbar$ and $d_{\rho,z}^{na} \equiv \langle n|d_{\rho,z}|a\rangle$. The appearance of imaginary frequencies in this formula is at first sight surprising but the advantage of this form is that $(\varepsilon(\mathrm{i}\xi)-1)/(\varepsilon(\mathrm{i}\xi)+1)$ is real, decreasing monotonically

from a positive value at $\xi = 0$ to zero at $\xi = \infty$ (Landau & Lifshitz 1980) so the integral is well behaved. For an almost-perfect mirror $\varepsilon(\mathrm{i}\xi) \gg 1$ up to frequencies far above the relevant atomic ones. In that case, we can recover equation (2.1), provided the atom is in its ground state, by making use of the identities

$$\frac{2}{\pi}\int_0^\infty \mathrm{d}\xi\, \frac{\omega_{na}}{\omega_{na}^2+\xi^2} = \mathrm{sgn}(\omega_{na}) \quad \text{and} \quad \sum_n |n\rangle\langle n| = 1.$$

For an excited state $|a\rangle$, there is another term in the energy which we have not considered until now. This has been worked out by several authors (for example, Wylie & Sipe 1985), who find that

$$\Delta E_{\mathrm{resonant}} = -\frac{1}{4\pi\varepsilon_0}\frac{1}{16z^3}\sum_n 2\,\mathrm{Re}\left(\frac{\varepsilon(\omega_{an})-1}{\varepsilon(\omega_{an})+1}\right)[|d_\rho^{na}|^2 + 2|d_z^{na}|^2]\Theta(\omega_{an}). \tag{3.3}$$

The Θ function means that only lower-lying states n contribute to the sum. Unlike the van der Waals interaction, which is a non-resonant effect, this interaction is due to the resonant emission and reabsorption of a photon of frequency $\omega = \omega_{an}$; in second-order perturbation theory, it corresponds to the terms in which the energy denominator is zero. This interaction is precisely analogous to the frequency shift of a classical oscillating dipole interacting with the in-phase part of its own reflected radiation field as discussed at some length by Hinds (1994). The total van der Waals shift of the atom is given by the sum of equations (3.2) and (3.3),

$$\Delta E_{\mathrm{vdW}} = \Delta E_{\mathrm{dispersion}} + \Delta E_{\mathrm{resonant}}. \tag{3.4}$$

When the mirror is a good reflector ($\varepsilon(\mathrm{i}\xi) \gg 1$), it is easy to show the rather marvellous result that equation (3.4) becomes nothing more than equation (2.1); the ground and excited state shifts follow the same simple Lennard–Jones formula.

The change in the spontaneous emission rate of the atom due to the presence of the surface is closely related to the resonant shift given in equation (3.3); in fact, they are the real and imaginary parts of the same coupling since the change in spontaneous emission is caused by the dipole interacting with the out of phase part of its own reflected field. Thus the change in decay rate for excited state $|a\rangle$ is

$$\Delta\Gamma = \frac{1}{4\pi\varepsilon_0}\frac{1}{16z^3}\sum_n \frac{4}{\hbar}\,\mathrm{Im}\left(\frac{\varepsilon(\omega_{an})-1}{\varepsilon(\omega_{an})+1}\right)[|d_\rho^{na}|^2 + 2|d_z^{na}|^2]\Theta(\omega_{an}). \tag{3.5}$$

The results we have collected here in equations (3.2)–(3.5) describe the changes in energy and spontaneous emission rate when an atom is placed sufficiently close to a thick slab of material. Here 'close' means that for every transition having an appreciable dipole strength d^{na}, the surface is in the near field of the dipole (i.e. $|\omega_{na}z/c| \ll 1$) and the electric field is just the gradient of an electrostatic potential. These results come from perturbation theory taken to order d^2 and it is assumed here that the temperature is low enough to neglect the thermal field.

Because the dispersive contribution to the van der Waals shift (equation (3.2)) is a broad-band non-resonant effect; it is not particularly sensitive to the spectral features in $\varepsilon(\omega)$. By contrast, the resonant effects $\Delta E_{\mathrm{resonant}}$ and $\Delta\Gamma$ are strongly enhanced when the dielectric constant at one of the atomic frequencies $\varepsilon(\omega_{na})$ has a value close to -1 because of the denominator $\varepsilon(\omega_{na})+1$ in equations (3.3) and (3.5). This naturally leads one to wonder what is happening in the material at $\varepsilon = -1$ to produce strong resonant coupling. The answer can be found by considering the

continuity of D_z, the normal component of the displacement field, across the surface of the material. Since $\varepsilon = 1$ outside the surface, the condition $\varepsilon = -1$ inside implies equal but opposite normal electric fields on the two sides of the surface, corresponding to a distribution of charge on the surface. Thus we can understand the strong effect at $\varepsilon(\omega_{na}) = -1$ as a resonance which occurs when the atomic dipole and the surface charge both oscillate at the same frequency.

The surface charge is caused by polarization of the medium. In a metal it is the electron gas that is polarized and the dielectric function can be approximated using the Drude model by

$$\varepsilon(\omega) = 1 - \frac{\omega_{\mathrm{p}}}{\omega(\omega + \mathrm{i}\gamma)}, \tag{3.6}$$

in which ω_{p} is the plasma frequency for the electron gas and γ is a phenomenological collision rate. The frequency of the surface wave (plasmon) is then just $\omega_{\mathrm{s}} = \omega_{\mathrm{p}}/\sqrt{2}$ if we ignore the damping. For a dielectric slab, we consider that $\varepsilon(\omega)$ at the frequencies of interest has a frequency-dependent part due to lattice polarization and a constant part due to electronic resonances at much higher frequency. In that case, we can write (Ibach & Lüth 1995)

$$\varepsilon(\omega) = \varepsilon_\infty + \frac{\omega_{\mathrm{T}}^2(\varepsilon_{st} - \varepsilon_\infty)}{\omega_{\mathrm{T}}^2 - \omega^2 - \mathrm{i}\gamma\omega}, \tag{3.7}$$

where ε_{st} and ε_∞ are constants and ω_{T} is the natural frequency of transverse oscillations in the bulk. Of course ε_∞, the high-frequency limit of this formula, is in fact only an intermediate value associated with the low-frequency wing of higher resonances which we ignore here; $\varepsilon(\omega)$ must tend really to unity at high frequency. When the damping is neglected, the frequency of the surface wave (polariton) given by the condition $\varepsilon(\omega_s) = -1$ is

$$\omega_{\mathrm{S}} = \omega_{\mathrm{T}}\sqrt{\frac{\varepsilon_{st} + 1}{\varepsilon_\infty + 1}}. \tag{3.8}$$

4. Spontaneous emission near a real surface

It is interesting to note that in the case of a perfect mirror $\mathrm{Im}[(\varepsilon(\omega_{eg})-1)/(\varepsilon(\omega_{eg})+1)]$ vanishes and according to equation (3.5) the spontaneous decay rate of the atom is unaffected by the surface. This seems to be at variance with the well-known result that an atom very close to a perfect reflector radiates either at twice the free space ratio or not at all, depending on the orientation of the dipole; a result which is obvious when we consider that the parallel dipole is cancelled by its image and the perpendicular dipole is doubled. This strong modification of the decay rate is missed in our near-field approximation because the field interacting with the atomic dipole is forced by our approximation to be exactly in phase with the dipole and therefore cannot remove energy from it, even in the limit where $z \to 0$ and the field becomes infinite. The doubling or vanishing of the decay rate close to a perfect reflector is in fact a retardation effect; the phase shift may be small but the field is correspondingly large and therefore causes a substantial alteration of the decay rate. What we see in equation (3.5) is something different which must be added to the retardation effect. Now there is a phase shift of the field caused by dissipation in the mirror and this contribution to the decay rate grows as $1/z^3$, in proportion to the field, because the phase angle does not vary with z.

From another point of view, we can consider this kind of dissipation as a new decay branch in which the atomic de-excitation is accompanied by the creation of a surface plasmon or polariton through the Coulomb interaction. The frequency of the atomic transition does not have to be identical to that of the surface excitation because of the damping characterized by γ in equations (3.6) and (3.7), but of course the coupling is strongest when the frequency mismatch is less than γ.

Let us consider an atom in excited state $|a\rangle$ close to a slab of material (the mirror). For simplicity we will suppose that the excited atom is spherical so that the dipole terms in brackets in equation (3.5) can be written as $\frac{4}{3}|\boldsymbol{d}^{na}|^2$. Let us also recall that the spontaneous emission rate on the $|a\rangle \rightarrow |n\rangle$ transition in free space is

$$\gamma_{an} = \frac{1}{4\pi\varepsilon_0}\frac{\omega_{an}^3}{\hbar c^3}\frac{4}{3}|\boldsymbol{d}^{na}|^2. \tag{4.1}$$

When these substitutions are made in equation (3.5), we are able to write the rate of decay into surface excitations very simply as

$$\Delta\Gamma = \sum_n \gamma_{an}\left(\frac{\delta_{an}}{z}\right)^3. \tag{4.2}$$

The length δ_{an} is the distance from the surface where the decay $a \rightarrow (n + \text{surface excitation})$ is as rapid as the free-space $a \rightarrow n$ transition. It is given by

$$\delta_{an} = \frac{\lambda_{an}}{2\pi}\sqrt[3]{\frac{1}{4}\,\mathrm{Im}\left(\frac{\varepsilon(\omega_{an})-1}{\varepsilon(\omega_{an})+1}\right)}. \tag{4.3}$$

For an experimental study of this effect we cannot easily position the atoms much closer to the surface than about 1 μm, so it is natural for us to consider long wavelength transitions. For example, we have found that the 13S state of caesium is a suitable candidate with a 13S–12P transition wavelength of 57 μm, a spontaneous decay rate of $\Gamma_0 = 1.3 \times 10^6\ \mathrm{s}^{-1}$ (calculated by Theodosiou 1984) and a partial rate on the 13S–12P branch of $\gamma_0 = 6.4 \times 10^4\ \mathrm{s}^{-1}$ (calculated from Edmonds 1979). Above a gold surface, such as we have used in our previous experiments, the dissipative coupling is characterized by a length $\delta_{13\mathrm{S},12\mathrm{P}} = 160$ nm and therefore seems too weak to measure in our apparatus. Conductors with more loss are better able to damp the atom, but still the frequency mismatch between the atom and the surface plasmon suppresses the strength of the dissipative coupling to a metal. By contrast, the surface polariton frequencies of some ionic crystals are very close to the Cs(13S–12P) frequency resulting in a much stronger coupling. In figure 5*a*, we display the free space decay rates Γ_0 and γ_0 for a caesium atom in the nS state. We also show the spontaneous decay rates $\Delta\Gamma$ at a distance of 1 μm from various surfaces, which we have calculated from equations (4.2) and (4.3) using optical constants given by Palik (1985, 1991) and reproduced in table 1. The lines indicate the decay rates for a fictitious caesium atom without fine structure whose principal quantum number is continuously tuneable. These curves clearly exhibit the resonant behaviour of the atom–polariton coupling. The dots mark the specific frequencies corresponding to the fine structure transitions of a real caesium atom. Here we have had to take fine structure into account because the splitting is comparable with the width of the polariton, both being of order 200 GHz. There are of course two dots for each principal quantum number n corresponding to the two fine structure levels in the $(n-1)$P state, the one to the left being associated with $\mathrm{P}_{1/2}$. The expected transition rates

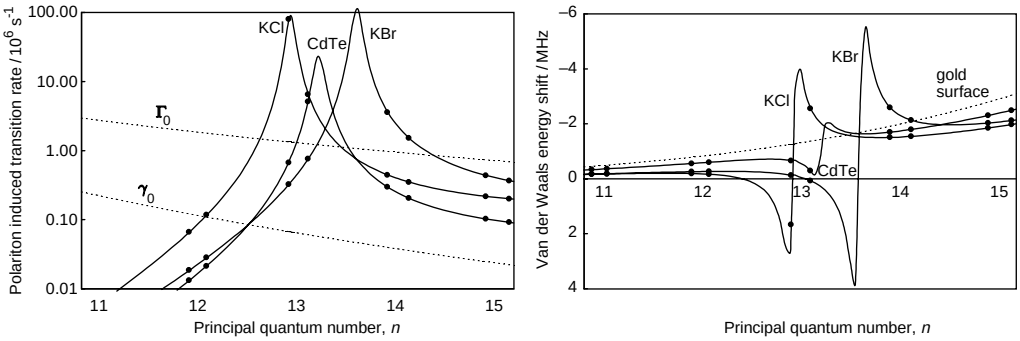

Figure 5. (Left) Polariton induced decay rates of caesium nS states 1 μm above various dielectric surfaces, calculated from equation (3.5) using the optical constants given in table 1. Γ_0: total free space decay rate, γ_0:$|n\mathrm{S}\rangle \rightarrow |n-1,\mathrm{P}\rangle$ rate. (Right) Corresponding van der Waals energy shifts calculated from equations (3.2)–(3.4). The two dots for each n correspond to the two $(n-1)$P fine structure levels. Expected decay rates and shifts are suitably weighted averages of the two values as listed in tables 2 and 3. The resonant behaviour of the atom–polariton coupling is evident in both graphs. Note that the van der Waals shift can go below the abscissa, indicating the possibility of a repulsive interaction.

Table 1. *Optical constants (defined in equation (3.7)) of various dielectric material*

optical constants	KCl[a]	CdTe[a]	KBr[b]
ω_{T} (cm^{-1})	140.8	140.7	113.5
γ (cm^{-1})	5.8	6.6	4.6
ω_{st}	4.3	9.5	4.3
ε_∞	2.2	6.6	2.2

[a]Taken from Palik 1985
[b]Taken from Palik 1991

$\Delta\Gamma$ in the real atom are averages of these values in which $\mathrm{P}_{3/2}$ has twice the weight of $\mathrm{P}_{1/2}$. These are listed in table 2. We see that the strongest effect is obtained with a KCl surface, which damps the 13S state of caesium at a rate of 31×10^6 s^{-1}, almost 500 times faster than γ_0 and more than 20 times Γ_0. Smaller but still quite significant enhancements are found for the 13S atom above CdTe and the 14S atom above Kbr.

5. Energy shift near a real surface

The resonant part of the van der Waals interaction energy $\Delta E_{\mathrm{resonant}}$ is given by equation (3.3). Once again it is convenient to characterize the atom–surface coupling by a length scale so that equation (3.3) becomes

$$\Delta E_{\mathrm{resonant}} = -\hbar\sum_n \gamma_{an}\left(\frac{\varepsilon_{an}}{z}\right)^3, \tag{5.1}$$

where

$$\varepsilon_{an} = \frac{\lambda_{an}}{2\pi}\sqrt[3]{\frac{1}{8}\,\mathrm{Re}\left(\frac{\varepsilon(\omega_{an})-1}{\varepsilon(\omega_{an})+1}\right)}. \tag{5.2}$$

Table 2. *Polariton induced decay rates of caesium nS states* 1 μm *above various dielectric surfaces, calculated from equation (3.5)*

(The optical constants given in table 1 are used. For comparison, we also show the total free space decay rate Γ_0 (taken from Theodosiou 1984) and the partial $|n, s\rangle \rightarrow |n-1, P\rangle$ rate γ_0 (Edmonds 1979).)

	polariton induced decay rate (10^6 s^{-1})			free space rate (10^6 s^{-1})	
n	KCl	CdTe	KBr	total rate Γ_0	partial rate γ_0
11	0.006	0.001	0.002	2.7	0.227
12	0.10	0.02	0.02	1.8	0.116
13	30.94	3.64	0.62	1.3	0.064
14	0.38	0.24	2.20	0.9	0.038
15	0.21	0.10	0.39	0.7	0.023

Table 3. *Van der Waals energy shift of caesium nS states* 1 μm above various surfaces, calculated from equations (3.2)–(3.4)

	van der Waals energy shift (MHz)			
n	KCl	CdTe	KBr	gold surface
11	−0.17	−0.35	−0.18	−0.48
12	−0.17	−0.59	−0.26	−0.81
13	−1.15	−0.41	0.004	−1.31
14	−1.53	−1.76	−2.28	−1.99
15	−1.93	−2.43	−2.09	−2.92

In figure 5*b*, the lines indicate the van der Waals shifts at a distance of 1 μm for a fictitious caesium atom without fine structure whose principal quantum number is continuously tuneable. These shifts are the sum of the gently varying term $\Delta E_{\text{dispersion}}$ given by equation (3.2) and the resonant shift. For $n = 13$, 14, one clearly sees the surface polariton resonances of KCl, CdTe and KBr, whereas the shift near a gold surface is featureless and indistinguishable from that of a perfect conductor. Once again, the dots in the figure 5*b* correspond to the two fine structure levels in the $(n-1)$P state and the expected van der Waals shift is the average in which the $P_{3/2}$ value has twice the weight of $P_{1/2}$. The values of ΔE_{vdW} are listed in table 3.

The main point to note in figure 5*b* is that the van der Waals attraction can be strongly affected by resonance with the surface polariton. There are regions where it is considerably stronger than the perfect conductor attraction and others where it is strongly suppressed or even becomes a repulsion, as indicated by a positive shift in figure 5*b*. The shifts predicted in our calculation are all attractive except for the very small positive shift at $n = 13$ with KBr. However, it may be possible to pull the frequency of one of these surface polaritons by doping the material, changing its thickness or structuring the surface in a suitable way. This would open the interesting

possibility of controlling the atom surface interaction, allowing us to make it strongly attractive, vanishing or repulsive at will.

6. Thermal effects

According to Fermi's golden rule, the spontaneous radiation rate is proportional to the square of the transition matrix element and hence to $\bar{n}+1$, where $\bar{n}$ is the mean number of photons per mode at the transition frequency. This number is given by Bose–Einstein statistics as

$$\bar{n}(\omega_{an}) = \frac{1}{\exp[\hbar\omega_{an}/kT]-1}, \tag{6.1}$$

a formula which applies to the surface polaritons of the last two sections as well as to the more usual fields of cavity QED. At room temperature, $\bar{n}+1$ is approximately 1.7 at the frequency of the caesium transition and we can therefore expect the spontaneous emission rates to be almost twice as large as we have calculated. Moreover, it will be possible to vary the thermal enhancement factor between 1.0 at 77 K (liquid N_2 temperature) and 3.0 at 613 K as a way of studying this effect in our laboratory.

In the same way, there should be a thermal enhancement of the resonant interaction energy $\Delta E_{\text{resonant}}$ allowing us to make this contribution to the total van der Waals energy up to three times as large as we have shown in figure 5*b*. By contrast, the temperature dependence of the non-resonant shift $\Delta E_{\text{dispersion}}$ is expected to be relatively weak. The net effect is that it should be possible to achieve a repulsive van der Waals interaction between a 13S caesium atom and KBr or CdTe surfaces which could be as large as several MHz and might well be observable in the laboratory.

References

Barton, G. 1987*a* Quantum-electrodynamic level shifts between parallel mirrors: analysis. *Proc. R. Soc. Lond.* A **410**, 141–174.

Barton, G. 1987*b* Quantum-electrodynamic level shifts between parallel mirrors: applications, mainly to Rydberg states. *Proc. R. Soc. Lond.* A **410**, 175–200.

Berman, P. R. 1994 *Cavity quantum electrodynamics*. New York: Academic.

Casimir, H. B. G. 1948 On the attraction between two perfectly conducting plates. *Proc. K. Ned. Akad. Wet.* **51**, 793.

Casimir, H. B. G. & Polder, D. 1948 The influence of retardation on the London–van der Waals forces. *Phys. Rev.* **73**, 360–372.

Drexhage, K. H. 1974 *Progress in optics 12* (ed. E. Wolf), p. 163. New York: North-Holland.

Edmonds, A. R., Picart, J., Tran Minh, N. & Pullen, R. 1979 *J. Phys.* B **12**, 2781–2787

Heinzen, D. J. & Feld, M. S. 1987 Vacuum radiative level shift and spontaneous-emission linewidth of an atom in an optical resonator. *Phys. Rev. Lett.* **59**, 2623.

Hinds, E. A. 1994 Perturbative cavity quantum electrodynamics. *Adv. Atom. Mol. Opt. Phys. Supp.* **2**, 1–56.

Ibach, H. & Lüth, H. 1995 *Solid-state physics*, 2nd edition, pp. 287–318. Berlin: Springer.

Jhe, W., Anderson, A., Hinds, E. A., Meschede, D., Moi, L. & Haroche, S. 1987 Suppression of spontaneous decay at optical frequencies—test of vacuum-field anisotropy in confined space. *Phys. Rev. Lett.* **58**, 666.

Lamoreaux, S. K. 1997 Demonstration of the Casimir force in the 0.6 to 6 μm range. *Phys. Rev. Lett.* **78**, 5–8.

Landau, L. D. & Lifshitz, E. M. 1980 *Statistical physics*, 3rd edn, part 1, pp. 377–384. Oxford: Pergamon.

McLachlan, A. D. 1963 Van der Waals forces between an atom and a surface. *Mol. Phys.* **7**, 381–388.

Palik, E. D. 1985 *Handbook of optical constants of solids*. New York: Academic.

Palik, E. D. 1991 *Handbook of optical constants of solids*, vol. II. New York: Academic.

Purcell, E. M. 1946 Spontaneous emission probabilities at radio frequencies. *Phys. Rev.* **69**, 681.

Sandoghdar, V., Sukenik, C. I., Hinds, E. A. & Haroche, S. 1992 Direct measurement of the van der Waals interaction between an atom and its images in a micron-sized cavity. *Phys. Rev. Lett.* **68**, 3432.

Sukenik, C. I., Boshier, M. G., Cho, D., Sandogdar, V. & Hinds, E. A. 1993 Measurement of the Casimir–Polder force. *Phys. Rev. Lett.* **70**, 560.

Theodosiou, C. E. 1984 Lifetimes of alkali-metal-atom Rydberg states. *Phys. Rev.* A **30**, 2881–2909.

Wylie, J. M. & Sipe, J. E. 1985 Quantum electrodynamics near an interface. *Phys. Rev.* A **32**, 2030.

PHILOSOPHICAL TRANSACTIONS OF THE ROYAL SOCIETY A MATHEMATICAL, PHYSICAL & ENGINEERING SCIENCES

PHILOSOPHICAL TRANSACTIONS OF THE ROYAL SOCIETY A MATHEMATICAL, PHYSICAL & ENGINEERING SCIENCES